IPSJ Transactions on Computer Vision and Applications Vol. 1 12–20 (Jan. 2009)

Regular Paper

Analyzing the Influences of Camera Warm-Up Effects on Image Acquisition

Holger Handel[†1]

This article presents an investigation of the impact of camera warm-up on the image acquisition process and therefore on the accuracy of segmented image features. Based on an experimental study we show that the camera image is shifted to an extent of some tenth of a pixel after camera start-up. The drift correlates with the temperature of the sensor board and stops when the camera reaches its thermal equilibrium. A further study of the observed image flow shows that it originates from a slight displacement of the image sensor due to thermal expansion of the mechanical components of the camera. This sensor displacement can be modeled using standard methods of projective geometry in addition with bi-exponential decay terms to model the temporal dependency. The parameters of the proposed model can be calibrated and then used to compensate warm-up effects. Further experimental studies show that our method is applicable to different types of cameras and that the warm-up behaviour is characteristic for a specific camera.

1. Introduction

In the last couple of years much work has been done on camera modeling and calibration [2),10),17),20)]. The predominant way to model the mapping from 3D world space to 2D image space is the well-known pinhole camera model. The ideal pinhole camera model has been extended with additional parameters to regard radial and decentering distortion [4),5),18)] and even sensor unflatness [7)]. These extensions have led to a more realistic and thus more accurate camera model (see Weng, et al.[18)] for an accuracy evaluation). Beside these purely geometrical aspects of the imaging process additional work has also been done on the electrical properties of the camera sensor and its influence on the image acquisition process. Some relevant variables are dark current, fixed pattern noise and line jitter [3),11),13)]. An aspect which has rarely been studied is the effect of camera warm-up on the imaging process. Beyer reports a drift of measured image coordinates to an extent of some tenth of a pixel during the first hour after camera start-up [1)]. Wong, et al. also report such an effect in Ref. 19) as well as Robson, et al. in Ref. 14). All of them only report drift distortions due to camera warm-up but do not give any further explanation of the origins of the observed image drift nor any way to model and compensate for these distortions. Today machine vision techniques have gained a great extension in many sensitive areas like industrial production and medical invention where errors of some tenth of a pixel in image feature segmentation caused by sensor warm-up can result in significant reconstruction errors. In Ref. 15) measurement drifts of an optical tracking system up to 1 mm during the first 30 minutes after start-up are reported. In many computer assisted surgery applications such reconstruction errors are intolerable. Thus, a better understanding of the impact of camera warm-up on the image acquisition process is crucial.

In this paper we investigate the influence of camera warm-up on the imaging process. We will show that the coordinates of segmented feature points are corrupted by a drift movement the image undergoes during camera warm-up. To our opinion this drift is caused by thermal expansion of the mechanical camera components which results in a slight change of the imaging geometry. We develop a model for the changing imaging geometry which can be used to compensate distortions in image segmentation during a camera's warm-up period. Finally, we provide further experimental results approving the applicability of our method.

The paper is organized as follows. Section 2 describes the experimental setup and the image segmentation methods from which we have observed the warm-up drift. Section 3 presents our model of warm-up drift and a way to calibrate the relevant parameters. Furthermore, a procedure is described to compensate for the image drift which fits easily in the distortion correction models widely used. Section 4 provides further experiments with different types of cameras.

2. Observing Warm-up Drift

This section describes the basic experimental setup and the image processing techniques which are used to investigate the effects of camera warm-up. The results of an initial experiment are described which are used to develop a math-

†1 Institute for Computational Medicine, University of Heidelberg, Germany

© 2009 Information Processing Society of Japan

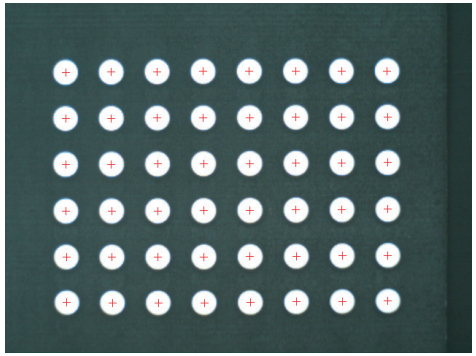

(a)

Fig. 1 Example for an image of the calibration pattern (taken by a VRmagic-C3 camera).

ematical model for the influence of camera warm-up.

2.1 Segmentation of Feature Points

To analyze the impact of temperature change after camera start-up a planar test field consisting of white circular targets printed on a black metal plate is mounted in front of a camera (equipped with a 640×480 CMOS sensor). The test pattern is arranged to cover the entire field of view of the camera and the complete setup is rigidly fixed. The center points of the targets are initially segmented using a threshold technique. The coordinates of the target centers are refined using a method described in Ref. 6). For each target the gray values along several rays beginning at the initial center are sampled until a gray value edge is detected. The position of the found edge is further refined to sub-pixel precision using moment preservation[16]. **Figure 1** (a) shows an example for a calibration pattern as it appears in the camera.

Next, an ellipse is fitted to the found sub-pixel edge points for each target using least squares optimization. The centers of the fitted ellipses are stored together with the current time elapsed since camera start-up. The segmentation process is continuously repeated and stopped after approximately 30 minutes. At the same time the temperature on the sensor board is measured. The obtained data basis has a temporal resolution of approximately three seconds.

2.2 Basic Results

Since the relative position between the test pattern and the camera is fixed the coordinates of the segmented target centers are not expected to vary systematically over time except noise. The results of the experiment are shown in **Fig. 2** and **Fig. 4**.

As one can clearly see from Fig. 2 (b) the segmented feature points do not stay fixed over time but are systematically displaced after the end of the warm-up period. Figure 4 displays a more detailed look into the observed displacement field. Figure 4 (a) shows the exact trajectory (the development of the $x-$ and $y-$coordinates over time) of the feature located in the top left corner of the image plane while Fig. 4 (b) displays the same for the feature located in the bottom right corner of the image plane. From these initial observations we can summarize some effects of camera warm-up:

- A drift of feature points can be observed during the camera's warm-up period.
- The observations correspond to the reports given in the literature (see especially 1)).
- The drift correlates with the measured temperature.
- Drift stops when camera temperature reaches thermal equilibrium.
- Drift is not uniform for complete sensor plane.
- The reason for the drift must originate in the camera or its mounting since the pattern is completely fixed and not exposed to temperature changes.

3. Modeling Warm-up Drift

Motivated by the initial results obtained from the experiment presented in the last section we claim that the observed flow field results from a movement of the image plane due to thermal expansion of the mechanical camera components. As one can see from Fig. 2 (a) the increase of temperature due to self-heating of the camera electronics can reach values up to of 15-20 K which can cause thermal expansion of the mechanical camera components. This expansion causes a change in the imaging geometry which in turn generates an optical flow of an observed static object in the image plane. The basic idea is to reconstruct this thermal induced camera motion analyzing the observed displacement of a known calibration device.

© 2009 Information Processing Society of Japan

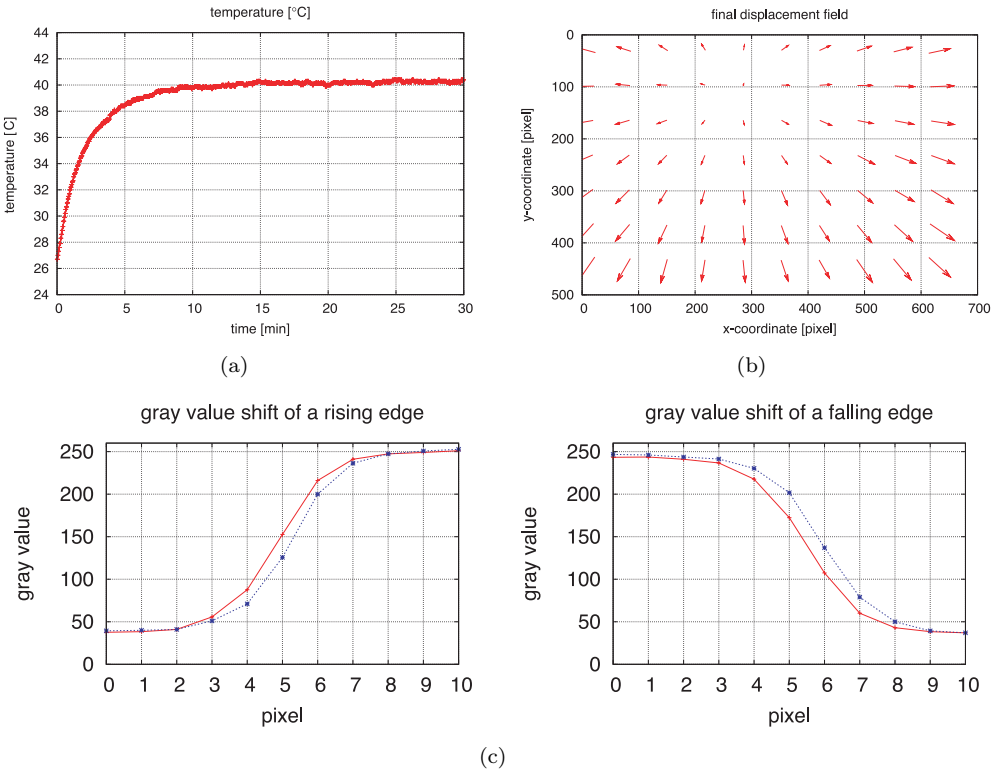

Fig. 2 Warm-up drift. Fig. 2 (a): Measured temperature on the sensor board. Fig. 2 (b): Total displacement from camera start-up until thermal equilibrium, the lengths of the arrows are scaled by a factor of 100. Fig. 2 (c): Gray value change for sampled line. The red curve shows the sampled gray values immediately after start-up and the blue curve after thermal stabilization. All data is taken by the VRmagic-C3 camera.

Taking the widely used pinhole camera model to describe the imaging process we can principally distinguish two cases:

- The thermal expansion of the sensor board affects only the image plane. The center of projection remains fixed (**Fig. 3** (a)).
- Both the image plane and the center of projection are displaced due to thermal expansion (Fig. 3 (b)).

Both cases can be found in real cameras. In the first case, the lens is fixed at the camera housing and is thus not affected by the local temperature increase of the sensor board since the distance to the board is relatively high. This configuration is typical for cameras equipped with C-mount lenses (see Fig. 3 (a)). In the second case, the lens holder is directly mounted on the circuit board. Thus, an expansion of the board displaces the lens and for this reason the center of projection (see Fig. 3 (b)). This configuration can be found at miniature camera devices used e.g. in mobile phones. Mathematically, the two cases have to be treated separately.

© 2009 Information Processing Society of Japan

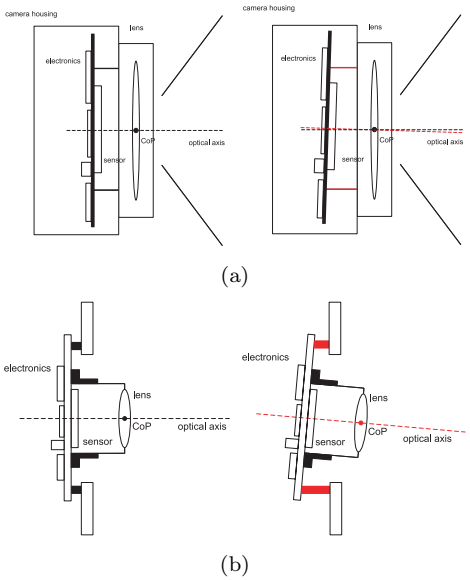

Fig. 3 Thermal expansion can cause displacement of the center of projection 3 (b) or not 3 (a).

In the remaining sections we use the following notation for the mapping from 3D world space to 2D image space:

$$\mathbf{x} = \mathbf{K}\,[\mathbf{R}|\mathbf{t}]\,\mathbf{X} \tag{1}$$

where $\mathbf{x} = (x, y, 1)^T$ denotes the homogeneous image coordinates of world point $\mathbf{X}$ also described by homogeneous coordinates. The camera is described by its internal parameters $\mathbf{K}$ with

$$\mathbf{K} = \begin{pmatrix} f_x & 0 & c_x \\ 0 & f_y & c_y \\ 0 & 0 & 1 \end{pmatrix} \tag{2}$$

The exterior orientation of the camera is given by the rotation $\mathbf{R}$ and the translation $\mathbf{t}$ (see Ref. 10) for details).

3.1 Fixed Center of Projection

If the center of projection remains fixed the observed optical flow will result from a movement of the image plane alone. In this case, the coordinate displacement can be described by a homography[10]. Let $\mathbf{x}(0)$ and $\mathbf{x}(t)$ denote the coordinates of the same target feature for the time $t = 0$, i.e. immediately after camera start-up, and an arbitrary time t. Then,

$$\mathbf{x}(0) = \mathbf{K}(0)[\mathbf{I}|\mathbf{0}]\mathbf{X}$$

$$\mathbf{x}(t) = \mathbf{K}(t)[\mathbf{R}(t)|\mathbf{0}]\mathbf{X} = \mathbf{K}(t)\mathbf{R}(t)\mathbf{K}^{-1}(0)(\mathbf{K}(0)[\mathbf{I}|\mathbf{0}]\mathbf{X}) = \mathbf{K}(t)\mathbf{R}(t)\mathbf{K}^{-1}(0)\mathbf{x}(0)$$

so that $\mathbf{x}(t) = \mathbf{H}(t)\mathbf{x}(0)$ with the time dependent homography $\mathbf{H}(t)$:

$$\mathbf{H}(t) = \mathbf{K}(t)\mathbf{R}(t)\mathbf{K}^{-1}(0) \tag{3}$$

Setting $\tilde{\mathbf{x}} = \mathbf{K}^{-1}(0)\mathbf{x}(0)$ we get $\tilde{\mathbf{H}}(t) = \mathbf{K}(t)\mathbf{R}(t)$. Since $\tilde{\mathbf{H}}(t)$ is invertible we can write

$$\tilde{\mathbf{H}}^{-1}(t) = (\mathbf{K}(t)\mathbf{R}(t))^{-1} = \mathbf{R}^{-1}(t)\mathbf{K}^{-1}(t) = \mathbf{R}^T(t)\mathbf{K}^{-1}(t) \tag{4}$$

Since $\mathbf{R}^T$ is orthogonal and $\mathbf{K}^{-1}$ is an upper diagonal matrix we can use QR decomposition to obtain $\mathbf{R}^T$ and $\mathbf{K}^{-1}$ once $\tilde{\mathbf{H}}^{-1}$ is given in Ref. 8). For a rotation by a small angle $\Delta\Omega$ around axis $\mathbf{l}$ we can further use the following approximation[12]

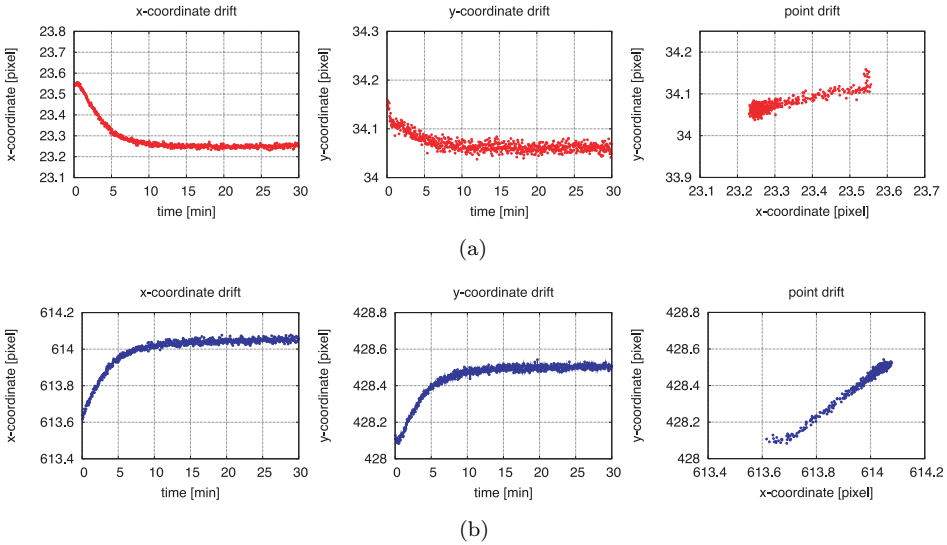

Fig. 4 Coordinate displacement. Coordinate changes of the top left target in Fig. 4 (a) and the bottom right one in Fig. 4 (b).

© 2009 Information Processing Society of Japan

$$\mathbf{R}(t) = \mathbf{I} + \mathbf{W}(t)\Delta\Omega(t) + O(\Delta\Omega^2), \tag{5}$$

where the matrix $\mathbf{W}(t)$ is given by

$$\mathbf{W}(t) = \begin{pmatrix} 0 & -l_3(t) & l_2(t) \\ l_3(t) & 0 & -l_1(t) \\ -l_2(t) & l_1(t) & 0 \end{pmatrix} \tag{6}$$

The vector $\mathbf{l}$ is a unit vector and thus has two degrees of freedom. We can identify the rotation by the three component vector $\tilde{\mathbf{l}} = \Delta\Omega\mathbf{l}$. From $\tilde{\mathbf{l}}$ we get $\Delta\Omega = \| \tilde{\mathbf{l}} \|$ and $\mathbf{l} = \tilde{\mathbf{l}} / \| \tilde{\mathbf{l}} \|$. The homography $\tilde{\mathbf{H}}(t)$ becomes

$$\tilde{\mathbf{H}}(t) = (\mathbf{K}(0) + \Delta\mathbf{K}(t))\mathbf{R}(t) \tag{7}$$

where $\Delta\mathbf{K}(t)$ denotes the time dependent offset to the original camera parameters and is given by

$$\Delta\mathbf{K}(t) = \begin{pmatrix} \Delta f_x(t) & 0 & \Delta c_x(t) \\ 0 & \Delta f_y(t) & \Delta c_y(t) \\ 0 & 0 & 0 \end{pmatrix} \tag{8}$$

Thus, $\tilde{\mathbf{H}}(t)$ is determined by seven time dependent parameters, namely $\Delta f_x(t)$, $\Delta f_y(t)$, $\Delta c_x(t)$, $\Delta c_y(t)$, the changes of the internal camera parameters and $\tilde{l_1}(t)$, $\tilde{l_2}(t)$, $\tilde{l_3}(t)$, the external orientation. Motivated by the results of our empirical studies (see Section 4 for further details) we choose bi-exponential functions for the time dependent parameters:

$$f(t) = a_0(1 - e^{-k_1 t}) + a_1(1 - e^{-k_2 t}) \tag{9}$$

The parameterization of $f(t)$ is chosen in such a way that $f(0) = 0$ and thus $\mathbf{H}(0) = \mathbf{I}$. Since $f(t)$ is determined by the four parameters a_0, a_1, k_1, k_2 and we have seven time dependent parameters for $\tilde{\mathbf{H}}(t)$ the complete warm-up model comprises 28 parameters. In Section 4 it is shown that the total number of parameters can be reduced in practice.

3.2 Moving Center of Projection

In this case we use the simplifying assumption that the center of projection and the image plane are equally translated, i.e., the internal parameters of the imaging device remain constant during the warm-up period. This assumption will later be justified empirically. Then, we get the following relations

$$\mathbf{x}(0) = \mathbf{K}\,[\mathbf{I}|\mathbf{0}]\,\mathbf{X}$$
$$\mathbf{x}(t) = \mathbf{K}\,[\mathbf{R}(t)|\mathbf{t}(t)]\,\mathbf{X}$$

Since the observed targets lie on a plane one can set $\mathbf{X} = (x, y, 0, 1)^T$ without loss of generality and hence the image coordinate changes can again be described by a homography (see Ref. 20) for a strict treatment).

$$\mathbf{x}(t) = \mathbf{K}\,[\mathbf{r_1}(t)\ \ \mathbf{r_2}(t)\ \ \mathbf{t}(t)]\,\tilde{\mathbf{x}}(0) \tag{10}$$

where $\mathbf{r}_i(t)$ denotes the i-th column of $\mathbf{R}(t)$ and $\tilde{\mathbf{x}}(0) = \mathbf{K}^{-1}\mathbf{x}(0)$. Thus, we get $\mathbf{H}(t) = \mathbf{K}\,[\mathbf{r_1}(t)\ \ \mathbf{r_2}(t)\ \ \mathbf{t}(t)]$. Given the homography $\mathbf{H}(t)$ the external parameters can be computed as follows [20]

$$\mathbf{r}_1 = \lambda\mathbf{K}^{-1}\mathbf{h}_1$$
$$\mathbf{r}_2 = \lambda\mathbf{K}^{-1}\mathbf{h}_2$$
$$\mathbf{r}_3 = \mathbf{r}_1 \times \mathbf{r}_2$$
$$\mathbf{t} = \lambda\mathbf{K}^{-1}\mathbf{h}_3$$

with $\lambda = 1/ \| \mathbf{K}^{-1}\mathbf{h}_1 \|$. Using the axis angle notation for the rotation $\mathbf{R}(t)$ we get six temporal dependent parameters, namely the three rotation parameters $\tilde{l_1}(t)$, $\tilde{l_2}(t)$, $\tilde{l_3}(t)$ as well as the three translational parameters $t_1(t)$, $t_2(t)$, $t_3(t)$. Again, we use bi-exponential terms to describe the temporal behaviour of the parameter values. Thus, we have 24 parameters.

3.3 Warm-up Model Calibration

In the previous sections we have shown how to model the coordinate displacement of segmented image features during camera warm-up. We now outline an algorithm to calibrate the parameters of the models:

(1) Determine the internal camera parameters using a method described in Refs. 20) or 17) based on a few images taken immediately after camera start-up. The obtained values are used for $\mathbf{K}(0)$ or $\mathbf{K}$ respectively.
(2) Collect image coordinates by continuously segmenting target center points.
(3) For each segmented image determine the homography $\mathbf{H}(t)$ (see Refs. 10), 12))
(4) Use a factorization method described in Section 3.1 or 3.2 depending on the type of camera to obtain values for the internal/external parameters.
(5) Fit a bi-exponential function to the values of each camera parameter.
(6) Perform a non-linear least squares optimization (e.g., Levenberg-Marquardt

© 2009 Information Processing Society of Japan

algorithm) over all 28(24) parameters minimizing the following expression

$$\sum_{j=1}^{M}\sum_{i=1}^{N} \parallel \mathbf{x}^j(t_i) - \mathbf{H}(t_i;\beta)\mathbf{x}^j(0) \parallel^2 \quad (11)$$

where M denotes the number of feature points and β the current parameter vector.

3.4 Warm-up Drift Compensation

With a calibrated warm-up model we can regard the influences of the sensor warm-up on the imaging process. For cameras whose center of projection remains fixed an image coordinate correction is straightforward. Given observed image coordinates $\mathbf{x}_o$ at time t after camera start-up the undistorted image coordinates $\mathbf{x}_u$ can be computed by multiplying with the inverse of $\mathbf{H}(t)$

$$\mathbf{x}_u = \mathbf{H}^{-1}(t)\mathbf{x}_o \quad (12)$$

This correction is independent from the structure of the scene, i.e., the distance of the observed world point from the camera. **Figure 5** (c) shows the results of this drift correction. In the second case, where the center of projection is not fixed, a direct correction of the image coordinates is not possible in general since the image displacement of an observed feature point depends on its position in the scene. In this case, the drift model can only be applied in reconstruction algorithms where the position of the camera is corrected accordingly.

4. Experimental Results

This section presents experimental studies which justify the applicability of the proposed warm-up model. The experiment described in Section 2 is conducted for two different types of cameras. The one is a VRmagic-C3, a miniature sized camera whose lens is directly mounted on the circuit board. The camera is equipped with a CMOS based active pixel sensor. The other camera is a SonyFCB-EX780BP, a CCD-based camera whose lens is not directly connected to the sensor circuit board. The initially estimated motion parameters are shown in Fig. 5. As the figures show, our choice for a bi-exponential function describing the temporal dependence of the camera parameters seems reasonable. Furthermore, one can see that for some camera parameters a simple exponential term is sufficient reducing the total number of parameters. Figure 5 (b) and **Fig. 6** (b) show the applicability of the chosen models to explain the observed image displacement. Figure 5 (d) shows the histogram for the errors between the observed image coordinates and the predicted ones for the Sony camera and Fig. 6 (c) shows the same for the VRmagic camera. **Table 1** and **2** show the parameters of the corresponding error histograms. The remaining errors are nearly Gaussian or Super-Gaussian distributed. Figure 5 (c) shows the results of the drift correction described in Section 3.4.

Table 1 Error statistics for the SonyFCB-EX780BP.

	Mean	Std.-Deviation	Kurtosis
x	-3.0250 $\times 10^{-5}$	0.0241	3.6251
y	-5.4138 $\times 10^{-5}$	0.0257	5.7161

Table 2 Error statistics for the VRmagic-C3.

	Mean	Std.-Deviation	Kurtosis
x	-6.717$\times 10^{-7}$	0.0079	7.5030
y	1.4355$\times 10^{-6}$	0.0083	15.6284

In a second experiment we examine the repeatability of the calibration. The drift model is repeatedly calibrated for one camera. The data has been collected over several weeks. **Table 3** shows the resulting parameters. The table contains the values of the motion parameters when the camera comes to a thermal equilibrium. The results show that the warm-up behaviour is characteristic for a specific device since the deviations between the parameters are quite small.

5. Conclusion

We have presented a study of the impact of camera warm-up on the coordinates of segmented image features. Based on experimental observations we have developed a model for image drift and a way to compensate for it. Once the warm-up model is calibrated for a specific camera we can use the parameters for drift compensation. The formulation of our displacement correction fits well in the widely used projective framework used in the computer vision community. Thus, the standard camera models used in computer vision can easily be extended to regard for warm-up effects. Further experimental evaluations have shown that

© 2009 Information Processing Society of Japan

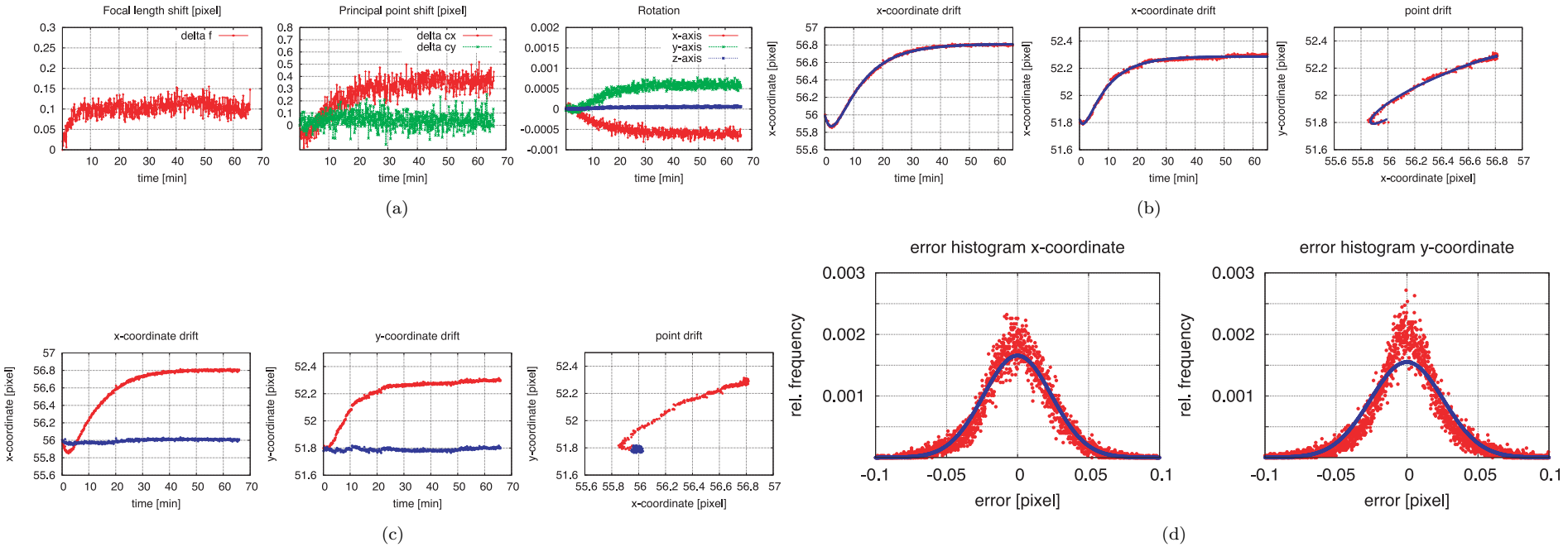

Fig. 5 Experimental results for the SonyFCB-EX780BP camera. Estimated internal and external parameters over time (Fig. 5 (a)). Figure 5 (b) shows the results of the drift calibration. The red curve depicts the segmented image coordinates and the blue one the ideal trajectory according to the calibrated drift-model. Figure 5 (c) shows the results of the drift compensation and Fig. 5 (d) shows the observed error distribution compared to the corresponding ideal Gaussian distribution.

Table 3 Camera motion parameters for a single camera (VRmagic-C3, CMOS) obtained from repeated experiments.

	Translation [mm]			Rotation				Residuals
	t_x	t_y	t_z	l_x	l_y	l_z	$\Delta\Omega$	RMSE
1	0.0095	0.0362	−0.2302	−0.9672	0.2542	-5.226×10^{-6}	4.175×10^{-5}	0.0114
2	0.0072	0.0367	−0.2297	−0.9812	0.1932	-4.028×10^{-6}	4.170×10^{-5}	0.0116
3	0.0057	0.0372	−0.2265	−0.9885	0.1515	-3.141×10^{-6}	4.196×10^{-5}	0.0119
4	0.0042	0.0369	−0.2248	−0.9937	0.1124	-2.383×10^{-6}	4.144×10^{-5}	0.0120
5	0.0052	0.0368	−0.2281	−0.9903	0.1387	-2.917×10^{-6}	4.148×10^{-5}	0.0115
μ	0.0064	0.0368	−0.2279	−0.9842	0.1700	-3.539×10^{-6}	4.167×10^{-5}	
σ	0.0021	0.0004	0.0023	0.0105	0.0554	1.114×10^{-6}	2.121×10^{-7}	

© 2009 Information Processing Society of Japan

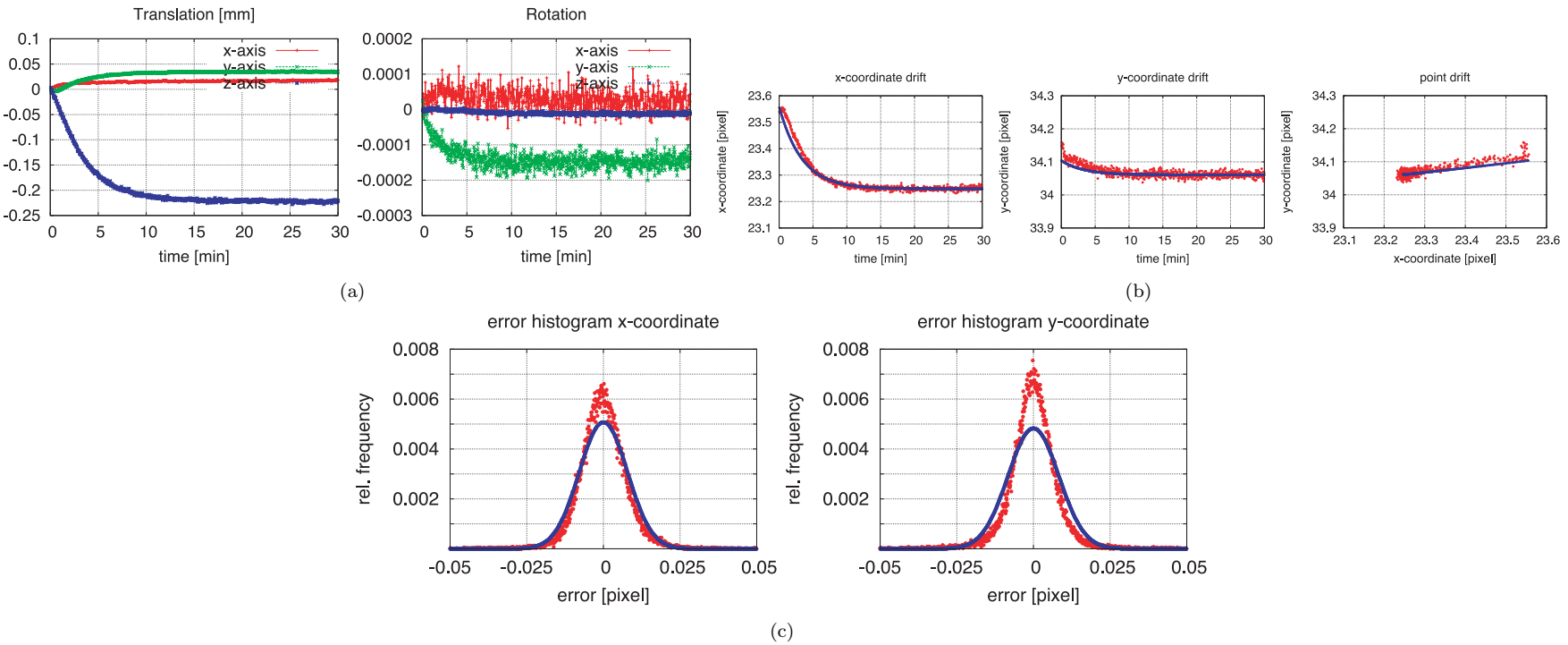

Fig. 6 Experimental results for the VRmagic-C3 camera. Estimated external camera parameters over time (Fig. 6 (a)). Figure 6 (b) shows the predicted trajectories of the point coordinates (blue) compared to the observed ones (red). Figure 6 (c) shows observed error distribution compared to the corresponding ideal Gaussian distribution.

our warm-up model is principally applicable for all kinds of digital cameras and additionally that the warm-up behaviour is characteristic for a specific camera. In the future we plan to use cameras with an on-board temperature sensor to get direct access to the camera's temperature. The formulation of our model presented here is based on the time elapsed since camera start-up assuming that the temperature always develops similarly and that the ambient temperature does not change significantly which can often be assumed for most indoor applications. A direct measurement of the temperature instead of time will probably increase accuracy further.

References

1) Beyer, H.A.: Geometric and radiometric analysis of a CCD-camera based photogrammetric close-range system, Dissertation No.9701, ETH, Zürich (1992).
2) Brown, D.C.: Close-range camera calibration, *Photogrammetric Engineering*, Vol.37, No.8, pp.855–866 (1971).
3) Clarke, T.A.: A Frame Grabber Related Error In Subpixel Target Location, *The Photogrammetric Record*, Vol.15, No.86, pp.315–322 (1995).
4) Devernay, F. and Faugeras, O.: Straight lines have to be straight, *MVA*, Vol.13, No.1, pp.14–24 (2001).

© 2009 Information Processing Society of Japan

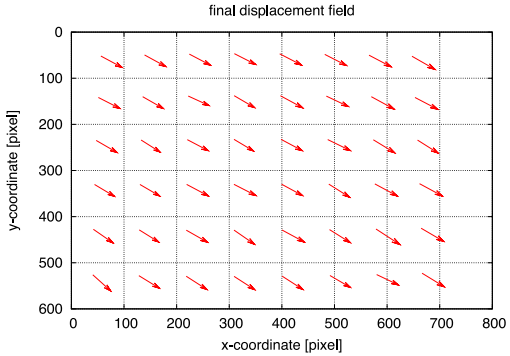

Fig. 7 Final displacement during camera warm-up for the SonyFCB-EX780BP. The lengths are scaled by a factor of 50.

5) El-Melegy, M. and Farag, A.: Nonmetric lens distortion calibration: Closed-form solutions, robust estimation and model selection, *Proc. ICCV*, pp.554–559 (2003).
6) Förstner, W. and Gülch, E.: A Fast Operator for Detection and Precise Location of Distinct Points, Corners and Centers of Circular Features, *ISPRS Intercommission Workshop on Fast Processing of Photogrammetric Data* (1987).
7) Fraser, C.S., Shortis, M.R. and Ganci, G.: Multi-sensor system self-calibration, *SPIE Proceedings*, Vol.2598, pp.2–15 (1995).
8) Golub, G.H. and VanLoan, C.F.: *Matrix computations*, Johns Hopkins University Press (1997).
9) Handel, H.: Analyzing the Influences of Camera Warm-Up Effects on Image Acquisition, *ACCV 2007*, Vol.4844, pp.258–268 (2007).
10) Hartley, R.I. and Zisserman, A.: *Multiple View Geometry in Computer Vision*, Cambridge University Press (2000).
11) Healey, G. and Kondepudy, R.: Radiometric CCD camera calibration and noise estimation, *PAMI*, Vol.16, No.3, pp.267–276 (1994).
12) Kanatani, K.: *Geometric Computation for Machine Vision*, Oxford University Press (1993).
13) Ortiz, A. and Oliver, G.: Radiometric calibration of CCD sensors: dark current and fixed pattern noise estimation, *IEEE International Conference on Robotics and Automation*, Vol.5, pp.4730–4735 (2004).
14) Robson, S., Clarke, T.A. and Chen, J.: Suitability of the Pulnix TM6CN CCD camera for photogrammetric measurement, *SPIE Proceedings, Videometrics II*, Vol.2067, pp.66–77 (1993).
15) Seto, E., Sela, G., McIlroy, W.E., Black, S.E., Staines, W.R., Bronskill, M.J., McIntosh, A.R. and Graham, S.J.: Quantifying Head Motion Associated with Motor Tasks Used in fMRI, *NeuroImage*, Vol.14, pp.284–297 (2001).
16) Tabatabai, A.J. and Mitchell, O.R.: Edge location to subpixel values in digital imagery, *IEEE transactions on pattern analysis and machine intelligence*, Vol.6, No.2, pp.188–201 (1984).
17) Tsai, R.Y.: A Versatile Camera Calibration Technique for 3D Machine Vision, *IEEE Journal for Robotics & Automation*, Vol.RA-3, No.4, pp.323–344 (1987).
18) Weng, J., Cohen, P. and Herniou, M.: Camera calibration with distortion models and accuracy evaluation, *IEEE Transactions on Pattern Analysis and Machine Intelligence*, Vol.14, No.10, pp.965–980 (1992).
19) Wong, K.W., Lew, M. and Ke, Y.: Experience with two vision systems, *Close Range Photogrammetry meets machine vision*, Vol.1395, pp.3–7 (1990).
20) Zhang, Z.: A Flexible New Technique for Camera Calibration, *IEEE Transactions on Pattern Analysis and Machine Intelligence*, Vol.22, No.11, pp.1330–1334 (2000).

(Received February 28, 2008)
(Accepted October 16, 2008)
(Released January 30, 2009)

(Communicated by *Tomas Pajdla*)

Holger Handel was born in 1980. He received his Diploma (equivalent to M.Sc.) in computer science in 2004 from the University of Mannheim. In 2005 he became Ph.D. student at the Institute for Computational Medicine (ICM) at the University of Mannheim which was transferred to the University of Heidelberg in 2008. His current research interests are the application of computer vision techniques in the field of computer assisted surgery (CAS), especially the accuracy evaluation and improvement of optical tracking systems used in medicine.

© 2009 Information Processing Society of Japan